DOI: 10.13009/EUCASS2023-463
Aerospace Europe Conference 2023 – 10TH EUCASS – 9TH CEAS

Architectural Trade-offs for a Hybrid-Electric Regional Aircraft

Philip Balack†, *Georgi Atanasov, Thomas Zill*

German Aerospace Center (DLR), Institute of System Architectures in Aeronautics, 21129 Hamburg, Germany,
philip.balack@dlr.de
† Corresponding Author

Abstract

Research entities and the aviation industry are collaborating to reduce the greenhouse gas emissions of the global aircraft fleet. To move away from fossil fuels as energy carrier while reducing the aircrafts primary energy demand are the ideal but challenging means to achieve this target. The research activities within the German government funded project TELEM have shown on a conceptual level that both measures could be realized for regional aircraft with an optimized hybrid-electric propulsion (HEP) architecture. Short, but very frequently flown distances of 200 nm and more could be served fully electrically by advanced propeller-driven aircraft with an assumed entry-into-service (EIS) in 2035. This paper gives an overview of integration concepts pursued in the project and reflects on various design aspects of a plug-in hybrid-electric aircraft, featuring a fully electric flight capability and a kerosene-fueled turboshaft range-extender. The aircrafts HEP architecture is optimized with regard to the number of propellers, as well as range extenders and their integration concept as to yield the best efficiency and to enable commonality with smaller aircraft leading to potential cost reductions among aircraft classes. Furthermore, a thermal management system, which is essential for the hybrid-electric propulsion architecture and its requirements are discussed and a favorable option selected. The final configuration features ten propellers and one range extender. The results also confirmed the exceptional efficiency of a plug-in HEP architecture for regional aircraft, showing a 34.6 % reduction in fleet energy and 64.4 % reduction in fuel consumption compared to a conventional turboprop architecture with an EIS in 2035.

Nomenclature

APU	Auxiliary Power Unit
DEP	Distributed Electric Propulsion
ECS	Environmental Control System
EIS	Entry-Into-Service
HEP	Hybrid-Electric Propulsion
HTP	Horizontal Tail Plane
MTOM	Maximum Take-off Mass
TAT	Turnaround Time
TMS	Thermal Management System
TLAR	Top-Level Aircraft Requirement
VCS	Vapor Cycle System
VTP	Vertical Tail Plane

1. Introduction

A synergistic aircraft integration strategy is the key requirement for hybrid-electric propulsion systems to be a viable option for future products. Many studies have been published on the optimal design of hybrid-electric propulsion architectures for regional and commuter aircraft. Variations of a parallel-hybrid electric architecture were identified by several authors to achieve a fuel burn reduction [1–5]. The serial hybrid-electric architecture was discarded by some authors mainly due to inefficiencies in the turbo-electric chain [1,4]. According to some studies of a parallel architecture, the minimum battery pack gravimetric energy density to achieve energy consumption parity with conventional aircraft amounts to about 500Wh/kg [1,5]. However, other studies, e.g., the one conducted by Spierling et al., identified a potential reduction in energy demand of 25% on a 250nm mission with a 425Wh/kg battery pack [3]. It is clear that the minimum energy density for energy parity with conventional aircraft and the question of the optimal architecture is heavily influenced by the many assumptions feeding into a study e.g., design range, hybridization concept, battery state-of-charge allowances, mass estimations and efficiencies of electrical machines and power electronics. However,

DOI: 10.13009/EUCASS2023-463

this study pursues a plug-in hybrid, i.e., a battery-electric concept with a kerosene-fueled gas turbine range extender, that can be applied to both parallel and serial hybrid-electric architectures. This concept was introduced for a parallel hybrid-electric architecture by Atanasov et al. on a commuter aircraft design in [6]. A more generic global potential assessment of the concept was provided by Atanasov in [7]. The configuration was further explored more in detail on a serial-hybrid approach by Atanasov, which was presented in [8]. A noise assessment study of a plug-in hybrid parallel versus a serial architecture was conducted by Balack[1] et al. in [9]. In the present study, a serial plug-in hybrid architecture is optimized in several trade-off studies with regard to the power providers (gas turbines, batteries) and thrust providers (propellers). Furthermore, the optimal wing integration i.e. high- or low-wing configuration is evaluated as the serial architecture combined with distributed propulsion enables new possibilities in this area. Additionally, the cooling demands and operating conditions of each of the hybrid-electric components are discussed. Special attention is payed to the battery thermal management system where various technologies are qualitatively compared and a suitable candidate selected. Finally, the optimized propulsion architecture is benchmarked against a conventional turboprop architecture in terms of fleet-level energy efficiency. The overall aircraft design is modelled with the tool *openAD*, which was introduced by Wöhler et al. [10]. The multi-disciplinary design process including mission and low-speed performance is managed in a RCE workflow [11]. The used data format is CPACS, which allows to standardize aircraft description, analyses and tool integration [12].

2. Baseline Aircraft

To enable a fair comparison between unconventional hybrid-electric and conventional technology, a baseline aircraft has been designed for a common set of top-level aircraft requirements (TLARs). Identical design parameters, e.g., gas turbine technology, wing aspect ratio, on-board systems etc., are applied to the baseline and to the hybrid-electric concept in order to ensure consistency. The baseline is similar to existing regional aircraft, in particular the ATR72. It features a high-wing configuration, a body-mounted landing gear, a T-tail and the turboprop engine integration on the wing. Figure 1 shows a three-view of the baseline concept.

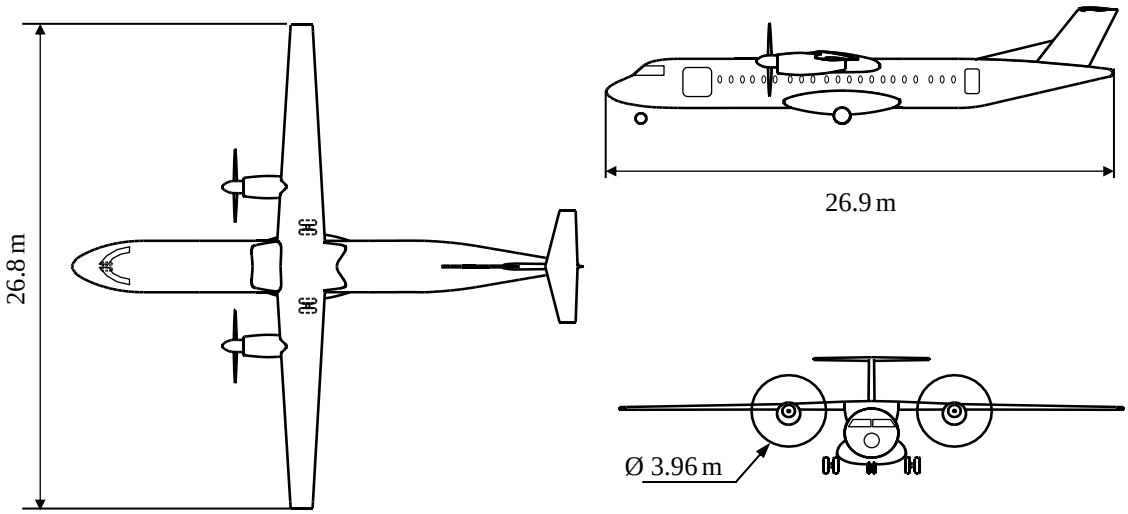

Figure 1: Three-view of the baseline aircraft

The hybrid-electric designs must power the aircraft systems in battery-only mode without bleed air from a thermal engine. In order to not distort the effects on aircraft level, a bleed-less architecture with an electric environmental control system (ECS) was also selected for the baseline. A gas turbine was designed for a set of thrust requirements and then varied in size to enable a sensitivity study at aircraft level [13,14].

3. Battery-Electric Concept with a Range Extender

The hybridization of the power train occurs on two levels - on the one hand, the hybridization of the power providers, i.e. gas turbine and battery, and on the other hand, the hybridization of energy providers, i.e. the energies from kerosene and batteries. Earlier design studies of hybrid-electric aircraft for the regional sector have shown that maximizing the

[1] Né Wassink

DOI: 10.13009/EUCASS2023-463

share of electrical energy is the most promising way to significantly reduce total energy consumption [6–8]. This is enabled by expanding the range and operations via a gas turbine that can be turned on and off during flight [6–8]. This principle is shown as a power profile over the mission trajectory in Figure 2.

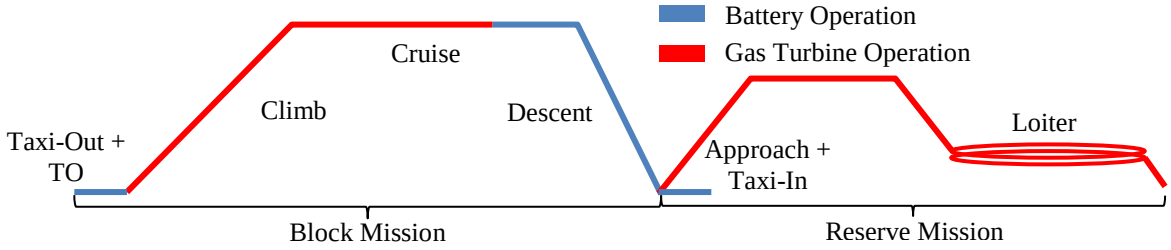

Figure 2: Flight- and hybridization profile for a fully battery-electric aircraft with a gas turbine acting as a range extender and enabler to perform the required reserve mission without using battery energy.

This assumes that the batteries are able to cope with all power requirements of normal and faulty flight conditions. With increasing size of the battery, the electric range and thus the share of fully-electric flight among the fleet increases too. Therefore, a larger battery also reduces the impact of the gas turbine efficiency on the fleet energy consumption. Ideally, the gas turbine is used only for the reserve mission or for range extension. This is the significant advantage over a purely battery-electric powertrain, where battery energy, which is expensive in terms of weight, also has to be used for the reserve mission. The overall concept is understood as plug-in hybrid and applied to all subsequent trade-offs.

4. Configuration Choice and Architecture Optimization

In the following paragraphs different variants of a serial-hybrid architecture are discussed. The criteria are primarily based on energy efficiency, as well as a qualitative cost assessment. The fully electric flight capability and turboshaft range extender imply a decoupling of power providers (gas turbine, battery) and thrust provider (propeller). Biser et al. have shown that an overall performance benefit can be leveraged when the thrust providers are distributed among the wing leading edge [15]. In the study, four additional propellers allowed for a 35 % reduction in the total installed propeller power versus a conventional twin-prop configuration [15]. Furthermore, distributed propulsion exhibits a positive effect on the wing at low speeds, which can generate more lift for the same area due to the larger blown area. The latter, in turn, allows the wing area to be reduced in order to operate at a more favorable wing loading during cruise flight. At least six propellers of the same size and power were considered for the serial-hybrid architecture. Due to the flexibility of the serial-hybrid coupling between power and thrust providers, the number of propellers and the number of gas turbines and their respective integration can be freely optimized.

4.1 Low-Wing Configuration

Distributed propulsion allows combining a large propeller disk area with small propeller diameter, which mitigates the propeller-ground clearance problems of a low-wing configuration. Therefore, a change from a high-wing to a low-wing configuration is beneficial, as this allows the landing gear to be integrated in the wing. Figure 3 shows a front view of both configurations.

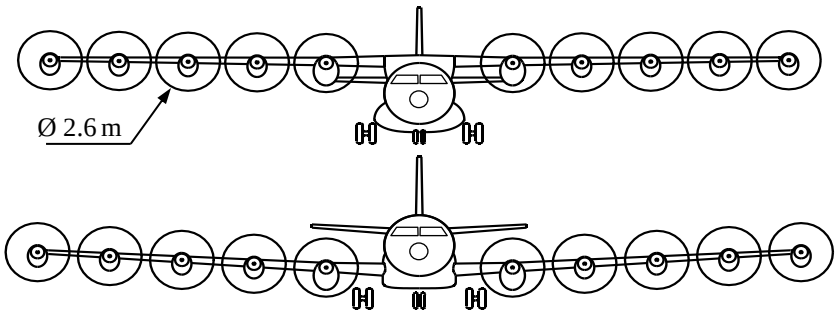

Figure 3: Front view of the high-wing configuration with body-mounted landing gear (top) and the low-wing configuration with wing-mounted landing gear (bottom)

This is useful from an aerodynamic and also structural point of view. The fuselage structure is relieved and thus lighter, since the load path of the heavy wing no longer goes through the fuselage frames as in the case of a high-wing configuration. In the following, the comparison between a low and a high-wing configuration is quantified, as it is a central

DOI: 10.13009/EUCASS2023-463

aspect of the aircraft concept. Figure 4 shows the influence of the individual configuration aspects on the total energy consumption of the aircraft on a typical block mission of 400 nm. First, the aerodynamic disadvantage of the high-wing aircraft with its fuselage-integrated landing gear becomes apparent. The required fairing increases the wetted area and the pressure (form) drag, resulting in an overall performance degradation of approximately 3 %. The wing attachment on the high-wing gives a minimal advantage in the effectiveness of the high-lift system, resulting in a wing that is about 5 % smaller and thus lighter. However, at aircraft level, this only translates to an advantage of about 0.3 % block energy reduction. A smaller wing normally results in a smaller empennage. Furthermore, the comparison showed a lighter main landing gear mass of the high-wing configuration, which is due to the sensitivity of the mass estimation method to the shorter landing gear length. The method does not distinguish between a wing and a body-mounted landing gear. Typically, body-mounted landing gears are heavier due to the inferior load path situation, but the calibration factor of the method was not adjusted for this comparison.

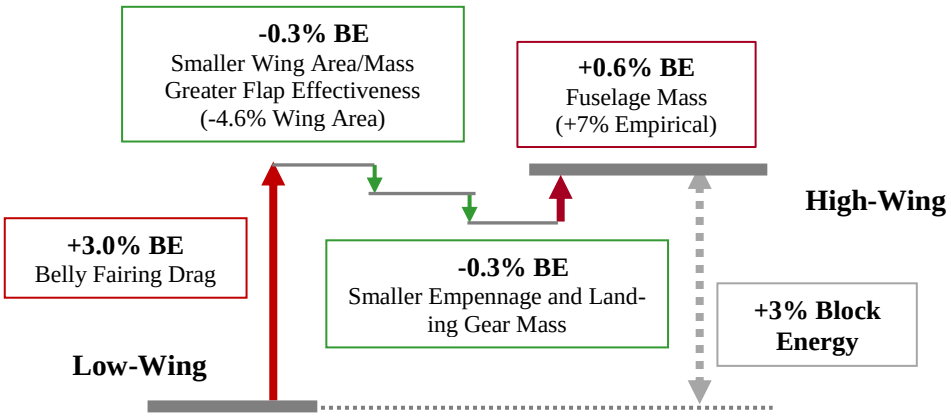

Figure 4: Configurational impacts on energy consumption on the 400nm mission.

Therefore, the landing gear mass will likely be higher, thus canceling the weight advantages of the smaller empennage. More importantly, though, the energy consumption is about 0.6 % higher due to the larger fuselage mass of the high-wing configuration. The wing mass including engines and batteries has a higher share in the total aircraft mass than usual for conventional high-wing aircraft. This additional load on the fuselage frames is not accounted for by the fuselage mass method and it is therefore considered optimistic. Despite the optimistic assumptions, the configuration effects result in an additional energy consumption of about 3.0 % at aircraft level. The condition for this comparison is the same number and diameter of propellers. The propeller diameter of the high-wing aircraft is rather limited by the wingspan than by the ground clearance as is the case for the low-wing, but with ten propellers there is little room for flexibility in this regard. In conclusion, the low-wing configuration not only gives a small advantage in overall performance but also adds other valuable benefits such as better safety characteristics in case of ditching. Furthermore, it relaxes some of the uncertainties regarding wing and fuselage structure weight. It should be kept in mind that the low-wing configuration is enabled by the small propeller diameters of the distributed propulsion.

4.2 Number of Propellers

To determine the optimal number of propellers, a configuration with a fixed battery pack was selected. The propeller diameter was kept constant for both configurations while allowing sufficient ground clearance and bank angle. Six and ten propellers were selected as variants for the parameter study. Six was defined above as the minimum number and ten is the maximum number that can still be accommodated on the given wing span with the selected diameter. The nacelles are sized according to the calculated battery volume of each nacelle. A front view of the comparison in shown in Figure 7. The calculations showed that the propeller power is sized by the takeoff distance requirement. The take-off performance was evaluated with the *LSperfo* tool developed by Fröhler [16]. In order to simplify the controllability of the aircraft during takeoff, it is assumed that in the event of a propeller failure, the same propeller on the opposite wing is automatically shut down too. Figure 5 shows the variation of the take-off lift coefficient at take-off safety speed (v2) and its influence on the total required propeller power of the aircraft. A notable result is the reduced total power for the 10-Prop variant compared to the 6-Prop variant with the same take-off lift coefficient. This reduction is due to the relatively smaller power loss in case of failure of two propellers compared to the 6-Prop variant. The take-off lift coefficients were optimized towards minimum block energy consumption. The lowest power-to-mass ratio does not yield the lowest block energy consumption. For the selected take-off lift coefficients (3.1 for the 6-Prop and 3.0 for the 10-Prop) a reduction in total power by 4.5 % is achieved with the ten propellers.

DOI: 10.13009/EUCASS2023-463

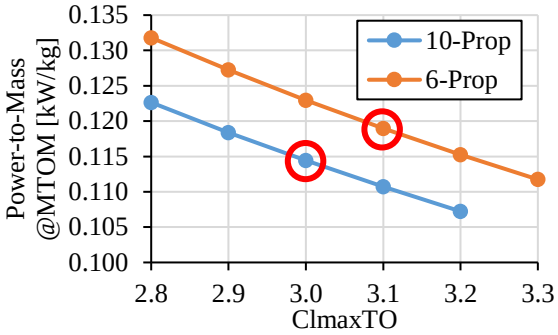

Figure 5: Impact of takeoff lift coefficient on the required total power-to-mass ratio (at the propeller).

Table 1 shows a comparison between the main wing and vertical tailplane (VTP) parameters and the propeller efficiency of the two variants. The distributed propellers improve the high-lift performance of the wing [15]. The wing area of the 10-Prop variant is 6% smaller, resulting a reduction of the structural wingspan by approximately one meter. However, the span including the tip propellers, is 1.6 m larger than on the 6-Prop variant. The lift coefficients in the landing configuration at 2.84 for the 6-Prop and with a moderate increase of 5.6 % at 3.0 for the 10-Prop were aligned by means of a top-down approach with the high-fidelity results from the study on distributed propulsion in [15]. The VTP volume coefficient of the 10-Prop was reduced by 12.5 % due to the relaxed one-engine inoperative condition at take-off. The higher decrease in reference area of 19.1 % is due to the fact, that the reduced wing area and reduced wing span feed into the calculation. This reduction is in line with a range of values obtained by the directional stability analysis conducted in [15]. The high installed propeller efficiency of 93.6 % in cruise condition is due to the low disk loading and positive installation interaction with the wing. This modelling is aligned with results of an optimized configuration with twelve propellers investigated by Keller [17]. The benefit in propeller efficiency of about two percentage points for the ten propellers versus the six propellers is a result of a low-fidelity actuator disc model implemented in *openAD*. However, a high-fidelity study for optimized propellers installed on the given wing geometry would be required to improve the credibility of this comparison.

Table 1: Comparison of geometrical and propulsion characteristics

Parameter		6-Prop	10-Prop	Diff [%]
ClmaxLanding	-	2.84	3.0	5.6
Wing Ref. Area	m^2	73.6	69.2	-6.0
VTP Ref. Area	m^2	8.1	6.5	-19.1
etaPropeller Cruise	%	91.7	93.6	2.1
Total Prop Shaft Power	kW	3939	3761	-4.5

Table 2 shows a mass breakdown comparison on aircraft and engine level. The lighter wing of the 10-Prop variant is noticeable. This is due to the smaller wing area and better wing-load relief due to more uniform engine mass distribution. The smaller wing also results in a smaller horizontal stabilizer. However, the overall engine mass increases slightly by 0.6 %. Together, this results in an approximately 0.9 % lighter structural mass and a 0.7 % lower maximum takeoff mass (MTOM). Overall, the design mission of 1000 nm results in a block energy reduction of 2.2 % for the variant with 10 propellers. Figure 6 shows an approximate breakdown of this figure into its individual effects at the aircraft level.

Table 2: Comparison Aircraft Level Mass Breakdown

Component	6-Prop	10-Prop	Diff	Component	6-Prop	10-Prop	Diff
	kg	kg	%		kg	kg	%
Wing	2625	2451	-6.6	Propellers	544	609	12.1
Fuselage Structure	2676	2676	0	Nacelles	516	525	1.7
HTP	325	296	-9.0	Mount Structures	562	566	0.6
VTP	128	99	-23.0	Gas Turbine	978	972	-0.6
Landing Gear	1243	1210	-2.7	E-Motors	461	440	-4.5
Engine	11810	11882	0.6	Generator	309	302	-2.2
Empty Weight	22142	21948	-0.9	Cables	62	85	36.5
Max. Fuel	5209	4734	-9.1	Cooling	122	119	-2.2
				Battery	8046	8054	0.1
				Gas Turbine Systems	210	210	0

DOI: 10.13009/EUCASS2023-463

The ten propellers are heavier than the six propellers, although they produce less total power. Here, a non-linear empirical function from Roskam [18], which was refitted with specific propeller masses, is used to determine the propeller mass. The ten nacelles have a slightly larger wetted area and thus a heavier fairing. Several component masses are linearly scaled with the nominal power, which makes the comparison work in favor of the variant with ten propellers. These include the electric motors, the power electronics and the cooling system. The variant with ten propellers is slightly more efficient. However, the level of detail of the methods and assumptions favors the latter.

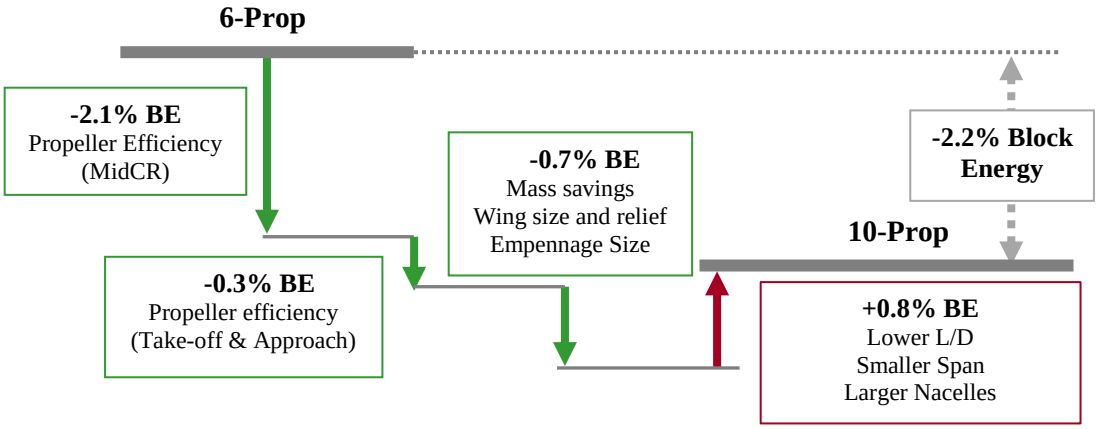

Figure 6: Configurational impacts on energy consumption on the 1000nm design mission.

Qualitatively, there is no huge advantage to be gained from increasing the number of propellers from six to ten. On the contrary, a more complex propulsion system is the result. Furthermore, maintenance effort and therefore cost increases with the number of parts to be maintained. Based on the previous remarks, a decision for the variant with six propellers would be the more favorable choice. However, in the context of the TELEM project, the decision was made for the ten propellers, as synergies can possibly be leveraged in conjunction with the 19-seater aircraft class in the area of research and development of electrical machines. The prospect of being able to install a drive train consisting of propeller, motor, power electronics and maybe an entire nacelle in several aircraft classes gives this variant a better industrial perspective.

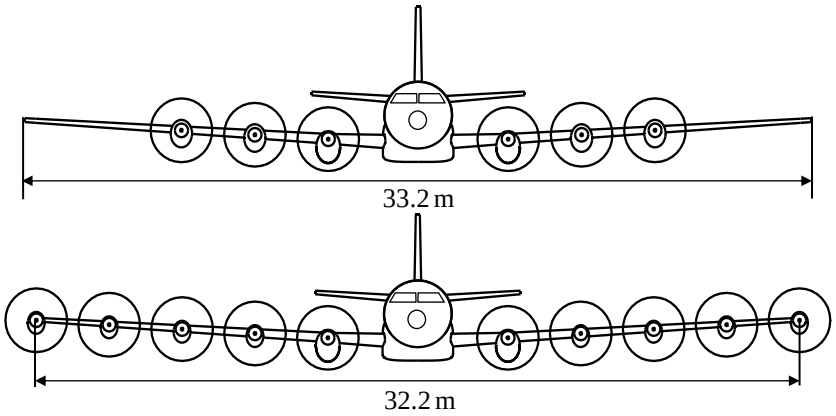

Figure 7: Front view of the variant with six (top) and the variant with ten propellers (bottom)

4.3 Number of Gas Turbines

The ability to fly the aircraft fully battery-electric allows the number of gas turbines to be reduced from the typical two to one. This is advantageous in terms of efficiency, mass and cost, as a single large gas turbine is lighter, more efficient and less expensive than two small ones providing the same shaft power. Figure 8 shows a bottom view on the schematic of the integration of a single gas turbine in the right-hand inner nacelle. The opposite nacelle is the same size for symmetry reasons and accommodates enough battery packs to balance the mass of the nacelle with the gas turbine. All other nacelles are equipped only with battery packs and have the same mass.

DOI: 10.13009/EUCASS2023-463

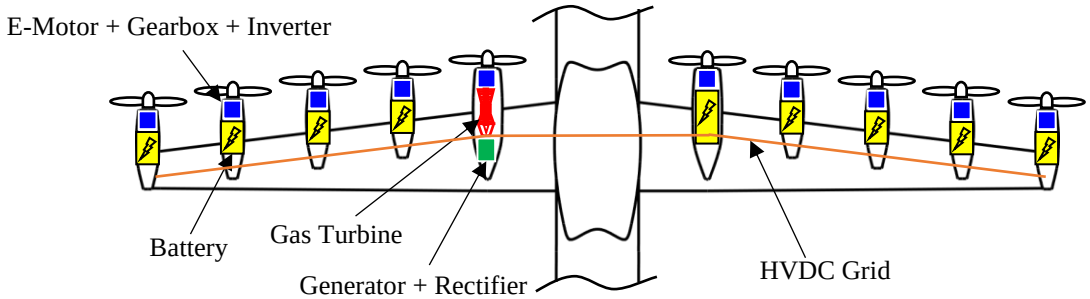

Figure 8: Bottom View: Integration of components on configuration with six propellers: single gas turbine in right-hand nacelle together with generator.

Flight planning can be adversely affected by a failure of the single gas turbine, since the achievable range to an en-route alternate airport can be longer with two redundant gas turbines compared to the battery-electric range. This disadvantage is illustrated in Figure 9.

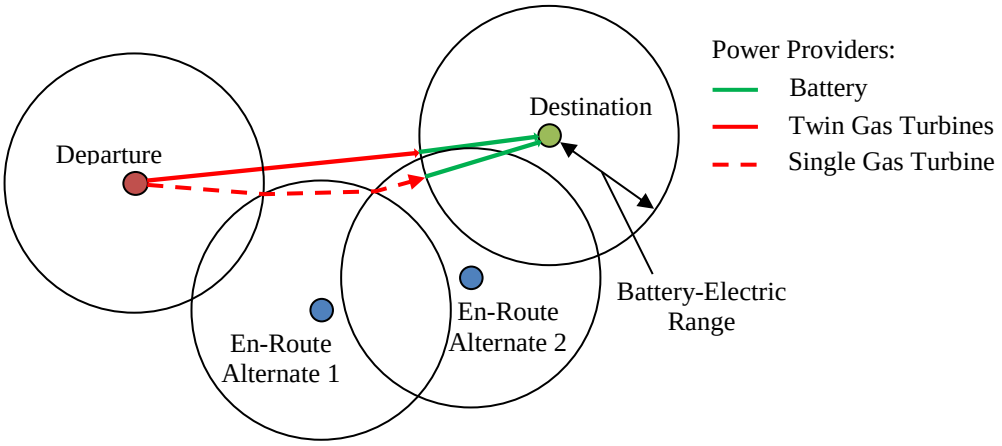

Figure 9: Increase in actual flight path with one instead of two gas turbines due to the limitation imposed by the battery-electric range.

However, according to Geiß et al. [19] the distance to an en-route alternate airport equipped with the required runway length in Europe in 99 % of cases is shorter than 68 nm and even shorter in the United States. In any case, the minimum battery-electric range of the investigated concepts was approximately 150 nm. Consequently, a single gas turbine would only prove disadvantageous in very sparsely populated areas. The block energy savings due to the single gas turbine are 2.0 % at 200 nm, 7.8 % at 400 nm, and 9.4 % at 1000 nm mission distances. The individual drivers are broken down in Figure 10 using the 400 nm mission as an example. In cruise flight, the single gas turbine is on average 8.6 % more efficient than two small gas turbines. However, the gas turbine is only used a certain fraction of the block time, so its added value is not fully exploited. Consequently, for lower energy hybridization levels, the configuration would benefit more from the single gas turbine. The results show that a single gas turbine is beneficial in terms of energy consumption. However, if the aircraft is on its way to a destination alternate airport, the battery energy is depleted and the single gas turbine fails, there is no way to continue level flight. Therefore, in that case the aircraft has to be landed with minimal hazard to the passengers and the environment. To the knowledge of the authors, there are no known certification rules that would prohibit such a procedure. Conventional twin turboprop also do not consider gas turbine failure during diversion for the fuel planning. Hence, a similar problem exists also with state-of-the-art aircraft.

4.4 Integration of a Single Gas Turbine

The integration of the single gas turbine in the inner nacelle gives multiple benefits on aircraft level: Short power cable lengths between generator and nacelles and the best accessibility for maintenance and overhaul. The proximity of the gas turbine to the fuel tank in the center and inner wing yields a lightweight fuel system. The systems are installed close to the total center of gravity of the aircraft. The installation in the nacelles enables more wing bending relief.

There are also some disadvantages to this configuration: A larger nacelle is needed to accommodate the gas turbine and the generator, resulting in an asymmetry compared to the other nacelles equipped only with batteries. The opposite nacelle, in which only batteries are accommodated, is not optimally utilized in terms of volume. For reasons of

DOI: 10.13009/EUCASS2023-463

symmetry and manufacturing, however, it makes sense to keep the overall size and to adjust only air inlets and outlets. The larger nacelles lead to a larger wetted surface, and thus more drag and slightly higher weight. Due to their length, the larger nacelles interrupt the trailing edge flaps, thus reducing the high-lift performance and leading to a disturbed flow around the nacelle, which results in an overall poorer aerodynamic efficiency. The asymmetric integration of the gas turbine and its thrust results in a small moment about the vertical axis that must be actively compensated for by either the control surfaces or by uneven thrust distribution among the propellers.

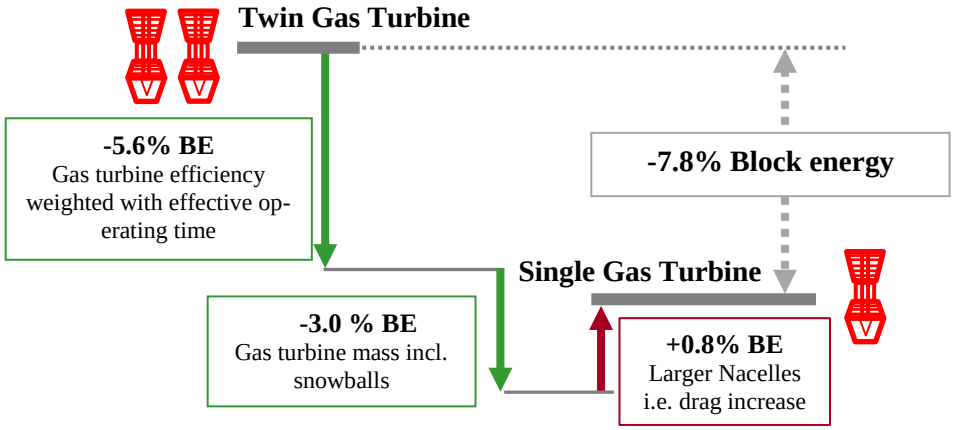

Figure 10: Disciplinary impact of a single gas turbine on the energy consumption on a 400nm mission with a configuration that enables 230nm battery electric range.

An alternative integration in the tail section of the fuselage was investigated in a simplified manner at aircraft level. Figure 11 gives an impression about the general installation concept. The advantages of this rearward integration are undisturbed and mechanically uniform trailing edge flaps with improved lift performance and identical nacelles with identical amount of batteries. The nacelles have a smaller wetted area and are also advantageous from an industrial point of view. The interchangeability of nacelles and the smaller certification effort are valuable benefits. Furthermore, the gas turbine provides symmetrical thrust in the direction of flight. A submersible inlet cowl could allow for more aerodynamically favorable integration when the gas turbine is not active.

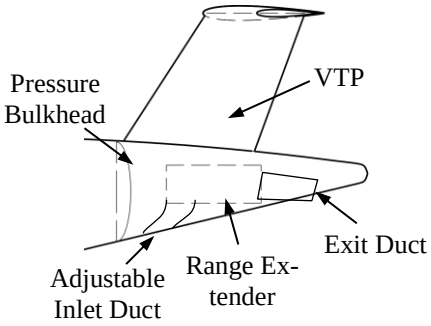

Figure 11: Integration of a range extender in the tail section of the fuselage

This integration comes also with some disadvantages though, such as longer power cables and a more complex fuel system. In the best case the range extender can be fitted in the unpressurized compartment between the pressure bulkhead and the horizontal tail plane. At worst though, a heavier T-tail has to be constructed to make room for the range extender. If the T-tail does not provide enough room, the fuselage length has to be increased, resulting in increased mass and aerodynamic penalty. Furthermore, a stronger inlet distortion in gas turbine duct is expected and therefore a worse compressor performance. Finally, the installed mass far from the overall aircraft center of gravity is never beneficial in terms of weight and balance.

A modified model was set up in order to provide an initial answer on the performance of a rear-integrated variant. The following assumptions were made for the trade-off:

- Constant battery mass
- Fuselage stretch of the center cross-section (at largest cross-section) by 0.5 m
- Shortening of the rear cargo compartment with increased width by 0.5 m due to hold the same amount of cargo

DOI: 10.13009/EUCASS2023-463

- Results in a total of 1 m more length for the integration of the gas turbine in the rear section
- Decrease in gas turbine efficiency by 0.5 % due to expected inlet distortion
- Additional fuel system mass of 210 kg (doubling the weight)
- Additional weight of 200 kg for adjustable inlet and outlet ducts for gas turbine flow
- Additional structural mass of 5 % for all cables towards the tail and components in the tail

Figure 12 shows an approximate component breakdown of the block energy increase of a tail-integrated gas turbine compared to a nacelle-integrated one. The added weight of the propulsion system is the main driver of the block energy consumption increase. The change to the T-tail and the fuselage extension are direct contributors to higher consumption. The latter offset the advantages of the smaller and more aerodynamically favorable nacelles.

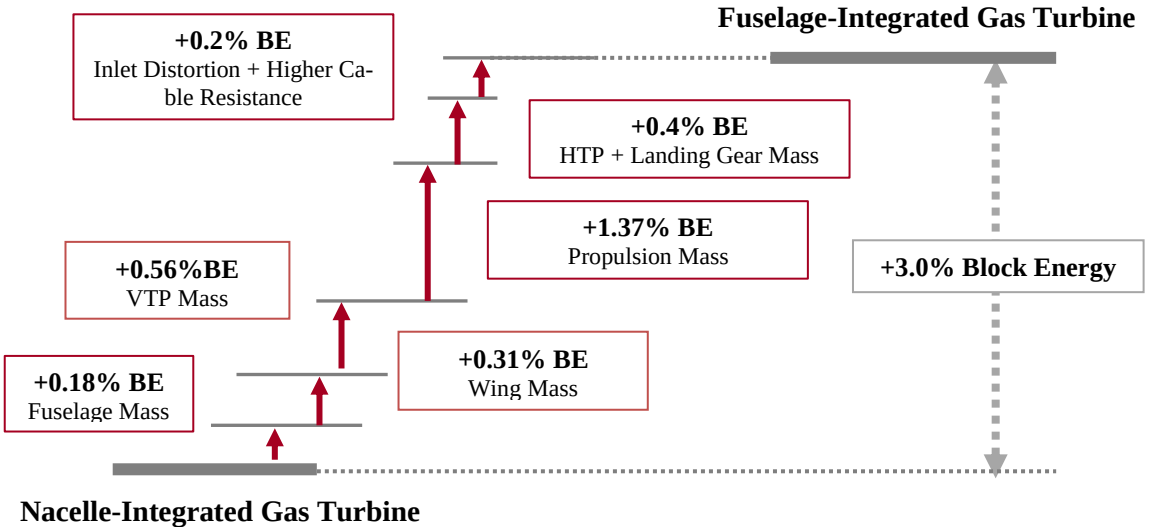

Figure 12: Impact of changed components from nacelle to fuselage integration of the gas turbine on the energy consumption on the 1000nm design mission.

The additional losses from higher cable resistance and higher inlet pressure drop are relatively small. The other effects are either snowball effects (HTP, landing gear, wing mass), whereby the wing structure mass also increases because of smaller wing bending relief due to the absence of the range extender mass. In Figure 13, the additional weight of the propulsion system of a tail integration of the gas turbine is visualized as a ladder chart.

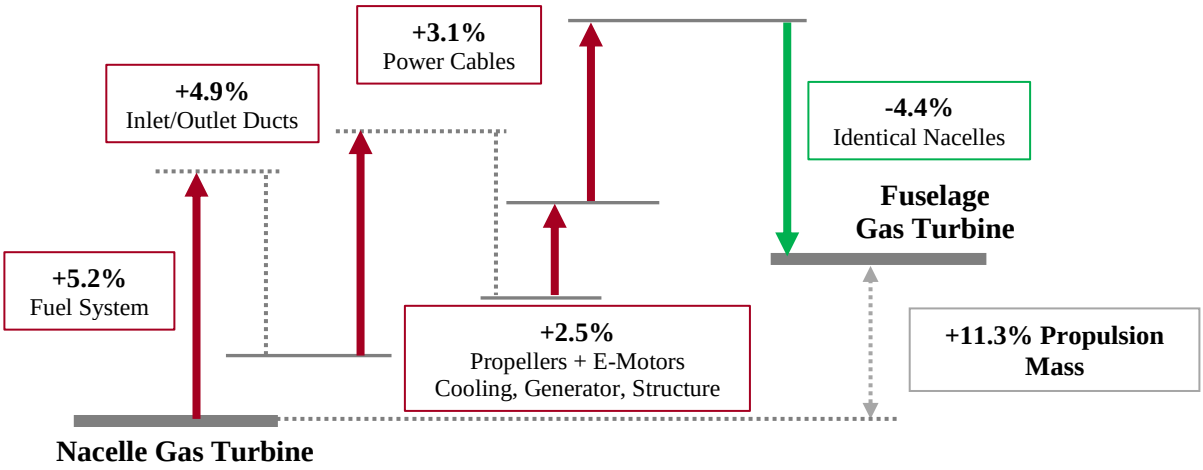

Figure 13: Breakdown of increase in weight among the engine components.

The main drivers of the mass increase are the longer fuel lines towards the rear of the fuselage, the more complex air ducting including adjustable inlets and outlets and the longer power cables from the generator to the nacelles. The 10 identical nacelles with smaller wetted surface and weight yield a reduction of 4.4 %. This is not enough to compensate for the mass increase due to the components mentioned above. In total, an engine mass increase by 11.3 % was calculated. The additional energy consumption of 3 % on aircraft level is not significant at this level of detail. However, it

DOI: 10.13009/EUCASS2023-463

indicates that such an integration does not yield benefits in terms of energy consumption. With more detailed investigation of the installation situation and optimization with respect to a short installation space of the range extender, it might be possible to relax the rather pessimistic assumptions. The industrial advantages of similar nacelles would be a good reason to choose the rearward integration. For an informed choice, more detailed analyses are needed.

4.5 Degree of Energy Hybridization

The degree of hybridization of the aircraft is hereinafter referred to as the energetic hybridization degree

$$H_E = \frac{E_{El}}{E_{Block}} \tag{1}$$

where E_{El} is the consumed electrical energy including discharge and charge losses and E_{Block} is the total energy consumption including the chemical energy bound in the kerosene. The degree of hybridization can be determined for a specific mission distance and also for a fleet distribution of missions. A plot of the fleet block energy reduction of the final HEP architecture with ten propellers and one range extender is given in Figure 14.

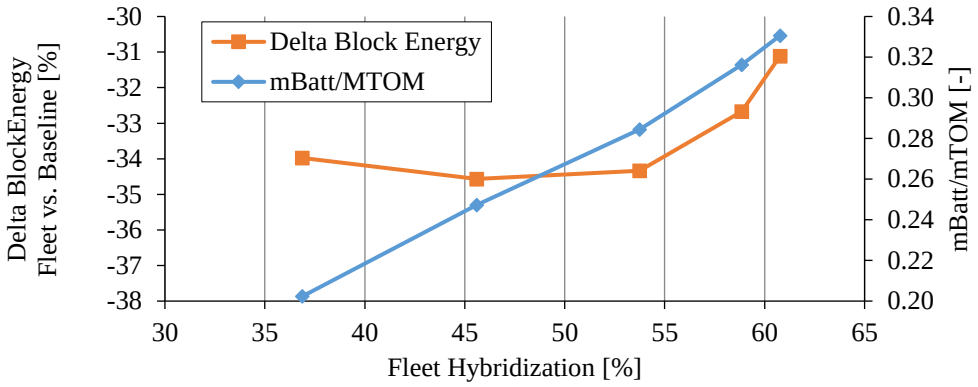

Figure 14: Fleet energy consumption benefit of a HEP architecture versus the baseline and increase in ratio of battery mass to aircraft mass dependent on the energetic fleet hybridization.

The underlying fleet mission mix is shown in Figure 18 and was provided by DLR internal market studies on regional aircraft. The aircraft is designed for a range of 1000nm with standard passenger payload. However, its performance should be evaluated on fleet level to reflect the real impact such an aircraft would have. The fleet mission mix, the underlying assumptions for the electric power train and the battery energy density critically impact the comparison to the baseline aircraft. The minimum hybridization i.e. size of the battery is given by the requirement that the battery alone can provide the maximum required power. The maximum required power is equal to the sum of the maximum required propulsion power plus the power required for the aircraft on-board systems. A cell type optimized for high energy density is intended for the battery. Therefore, the battery must have a minimum capacity at a fixed nominal discharge rate to deliver the required power. As the capacity increases, the instantaneous discharge rate for a given load on the battery decreases. Conversely, the discharge efficiency increases. However, this effect is yet neglected in the model. The maximum battery size is methodically more difficult to determine and essentially concerns the ability to integrate the batteries in nacelles and the overall cost trade-off. As the battery size increases, the wing is resized at iso-aspect ratio i.e. with increasing span. However, the 36 m box as a TLAR limits the wing span including the propellers. As can be seen in Figure 14, a minimum energy consumption is obtained for a hybridization level of about 45 %. The curve is relatively flat around the optimum. The steeper increase in energy consumption towards hybridization levels greater than 55 % is imposed by the wing box limit. Due to the limit the additional wing area is added at a decreasing aspect ratio, conversely increasing the induced drag.

The optimal choice of hybridization level also depends on the expected operating costs of the aircraft. In Figure 15, an energy cost comparison to the baseline is plotted for four different scenarios of energy cost. Each line represents a fixed ratio of fuel over electricity cost per kWh. At low fuel costs (1/4), the ideal hybridization level is the lowest one. This ratio is true for an exemplary fuel cost of approximately 600 $/t and 10 ct/kWh of electricity. For increasing fuel costs the lines approach a flat behavior. At this point the energy cost is a driving factor in a decision for an optimal hybridization level. At fuel costs half to those of electricity (1/2) a break-even between the unconventional HEP architecture and the conventional occurs. With relatively increasing fuel costs, the HEP architecture obviously gains and at cost parity between fuel and electricity per kWh, the HEP architecture achieves an overall energy cost reduction of up

DOI: 10.13009/EUCASS2023-463

to 35 %. For even higher ratios of fuel to electricity cost, the optimum hybridization level shifts to the largest battery packs.

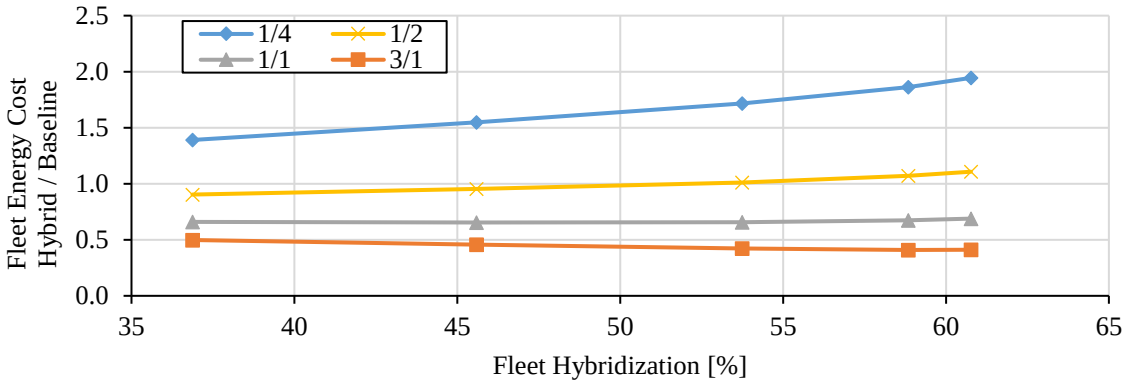

Figure 15: Fleet energy cost versus the baseline at four ratios of fuel over electricity cost per kWh. In blue: $/kWh fuel per $/kWh electricity = 1/4.

The future costs of sustainable aviation fuels and renewable energy are difficult to predict. Therefore, it is also difficult to draw a conclusion on the optimal hybridization level. Furthermore, the energy costs are an important factor, but not the only one. Larger batteries make the aircraft heavier and thus more expensive to purchase and to maintain. The higher replacement costs for larger batteries after a fixed number of cycles must be taken into account in a cost analysis. However, the lower discharge rates on larger batteries would improve battery life and should also be considered in the decision making. A detailed study on the cost impact of the hybridization level is out of the scope of this study.

4.6 Charging Strategy and Turnaround Time

There are two possible strategies for charging the battery before the flight: Either fast-charging by cable at the gate, or rapidly exchanging with already charged batteries. Table 3 describes various pros and cons of the two strategies. The success of battery-electric cars and also trucks comes with the development of suitable fast charging infrastructures, such as the one suggested by Starke et al. [20].

Table 3: Pros and Cons for cable charging and battery swapping

Cable Charging	Battery Swap
Pros	
• Less effort (no additional personnel) • Faster compared to battery swapping depending on number of power plugs • Fixed Battery integration allows lowest weight • Higher safety due to fixed internal connections	• Slower, more efficient charging at airport central infrastructure • Simplified cooling system as fast-charging is not considered • Possibly the fastest with a centralized battery pack
Cons	
• Expensive fast-charging infrastructure • Intermediate storage infrastructure required for the grid not to be overloaded at peak hours	• Special equipment required for handling of the large batteries • Large effort for decentralized battery packs • More personnel required for inspection of power connections (two-man rule) • Complex battery pack integration for quick release

Due to the expected technology maturity of these fast charging infrastructures and the advantages mentioned in Table 3, especially regarding the lower handling effort, fast charging of the batteries at the gate is assumed to be the optimal choice for charging large aircraft batteries. Similar to fuel trucks, a battery truck with additional cooling capacity on-board could be used to deliver the electric energy to each aircraft. These battery trucks can be charged at a centralized airport power plant that is connected to the grid, possesses intermediate energy storage capabilities and also utilizes available renewable energy sources at the airport. In a later stage and for larger loads, an additional underground network of power lines could be installed and used to charge multiple aircraft at the same time.

DOI: 10.13009/EUCASS2023-463

An operational risk that exists in connection with fast charging is the turnaround time. Appropriate turnaround time statistics for relevant regional aircraft were compiled DLR internally. Table 4 shows data from 13000 flights in scheduled service broken down by turnaround time. The share of 30 to 50 minutes turnaround time amounts to 49 % while occasions with greater than 50 minutes turnaround time amount to about 46 % of the flights. For an initial risk analysis, an average charging time of 30 minutes is assumed from 0 % to 80 % battery charge level. A fraction of the turnaround time is allocated for the battery charging process. Other processes, such as boarding and deboarding, baggage and catering handling should be performed simultaneously. Turnarounds with more than 50 minutes can be regarded as low risk because they allow 10 to 20 minutes of time for other handling processes. However, half of the turnarounds that last between 30 and 50 minutes could be adversely affected by a full battery charge. Thus, the 30 to 50 minutes is regarded as the critical scenario.

Table 4: Data on turnaround times of ATR72 and Dash-8 aircraft

TAT [min]	≤20	20<x≤30	30<x≤50	50<x≤60	>60
Share	1 %	5 %	49 %	18 %	28 %

A typical operation is a two-leg flight between two airports where the fuel tank is filled for the outgoing and the returning flight. The second turnaround is shorter as no fuel has to be tanked. Furthermore, it is assumed that only the first airport provides the fast-charging infrastructure. Thus, it is necessary to split the battery energy charged at the first airport among the two flights. If the turnaround time, especially the first, longer turnaround is critical for the operator to keep the slots at both airports, it might not be feasible to fully charge the battery. This would cause a drastic decrease in efficiency. This poses a risk for some operations; however, the real charging time of course depends on the battery technology and the airport infrastructure which is both difficult to predict as the technology is rapidly developing.

4.7 Generator Sizing

The generator can be either sized to match the entire envelope of the gas turbine or it can also be optimized to unusual requirements because the battery is already required to fulfill all thrust requirements of the envelope. The two typical requirements are the take-off and the top-of-climb operating point i.e. residual climb capability at initial cruise altitude with ISA Delta+10 °C. The gas turbine as the power provider is sized for top-of-climb, as is usually the case with turboprop engines. Furthermore, the gas turbine delivers more power at sea level than at top-of-climb. Therefore, the generator could be sized to that available sea-level power. However, the generator can also be sized for the minimum required power i.e. the available gas turbine output at top-of-climb ISA delta+0 °C, to save cost, weight and volume. If the generator is sized for take-off, it is about 15 % more powerful, and thus also heavier and more voluminous. However, due to the small share of the generator mass on aircraft level, this disadvantage is insignificant. The fleet evaluation also showed a 2.6 % reduction in energy consumption, as the faster climb capability allows for overall more efficient missions. The more powerful generator also allows a similar climb time to that of comparable regional aircraft. It was therefore decided to size the generator to the available sea-level power of the gas turbine.

4.8 Thermal Management System

The proposed hybrid-electric architecture consists of several components that have individual thermal management requirements. Electrical machines such as the motors and the generator operate at similar temperatures. However, they might run at different speeds and therefore allow individual cooling solutions. The power electronics i.e. the inverters and the rectifier operate at similar temperatures as the electrical machines. The battery typically operates in a much lower and narrower temperature spectrum than motors and power electronics and therefore requires a more complex thermal management. The power lines between the battery and the motor, and respectively, between the generator and the nacelles, are less critical in terms of thermal management. It is assumed that no active cooling is required as the outer wings are dry and ventilated. Figure 16 shows the general integration of the electrical components in the nacelles on the wing. Each of the outer nacelles contains a battery pack, an inverter and a geared electric motor. The generator power is distributed via several cables and fed separately to each nacelle through the wing box.

The e-motors and inverters operate at similar temperatures and are installed close together in order to minimize the length of AC cables. Therefore, it also makes sense to design a common cooling solution. For motors and inverters, two cooling solutions are basically possible: air or liquid cooling. The motor cooling option is constrained by the maximum speed of the motor. Since a geared, high-speed motor was selected, the choice was liquid cooling for both components. The cooling system mass was determined with the ratio of rejected heat to system mass given in Table 6. The cooling drag was assumed to be neutral for the current state of the computational model due to the high efficiency of the electric motor and inverter. Liquid cooling was also chosen for the generator and rectifier, as the generator is a high-speed machine too.

DOI: 10.13009/EUCASS2023-463

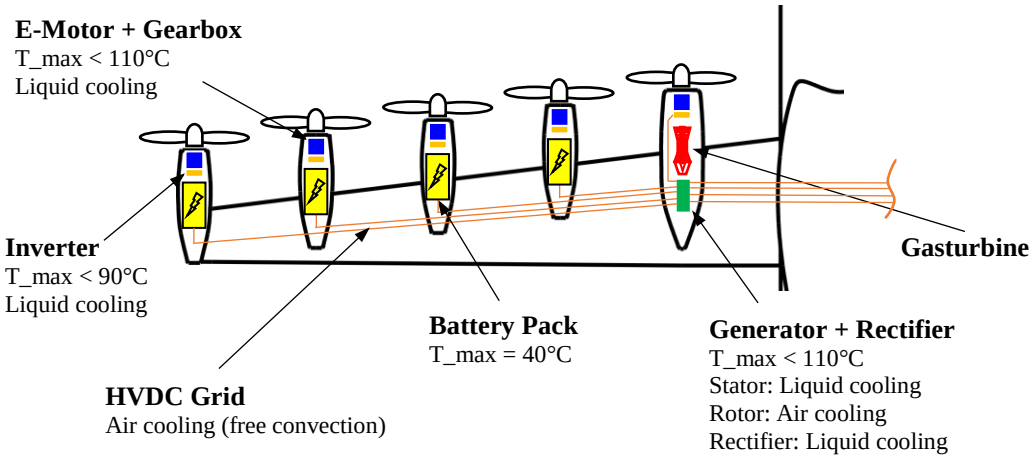

Figure 16: Electrical components and their maximum material temperatures (e-motor, inverter, generator, rectifier), respectively the maximum operating temperature of the battery.

The battery requires its own cooling solution, since it operates at significantly lower maximum temperatures than motors and inverters. Furthermore, a certain minimum temperature is required for operation in order to ensure safety and not to unnecessarily accelerate the aging of the cells. Ideally, therefore, not only cooling but also heating is required in order to operate at low temperatures. Battery cells can be cooled by air or a liquid medium. An example of air cooling from aviation is the Pipistrel Alpha Electro, a two-seat powered glider equipped with air-cooled battery packs [21]. However, the same company offers a similar aircraft with liquid cooled battery packs, the Pipistrel Velis Electro [22]. According to An et al. liquid cooling is more efficient overall, especially due to the higher thermal capacity of liquid cooling media, which also provide more safety during peak loads [23]. Liquid heat acquisition systems can differ substantially in their design in order to keep the additional weight as low as possible. Annapragada et al. have analyzed and evaluated different variants specifically for an aerospace application [24]. The best option achieved a weight reduction of more than 60 % compared to a baseline, which was based on the liquid heat acquisition system of the battery-electric Tesla Model 3 [24]. In this study, a maximum battery temperature allowance of 40 °C at ISA Hot Day conditions (ISA+30 °C=45 °C) was set. Due to the positive temperature gradient, the cooling system cannot cope without a heat pump on ground during fast charging. Depending on the thermal insulation and efficiency of the battery, heating of the liquid or gaseous coolant might be necessary during cruise at ambient temperatures of -38 °C.

Battery Cooling via the Environmental Control System

Battery-electric road vehicles are exposed to similar operating conditions to aircraft in terms of possible ambient temperatures. Typically, liquid-cooled battery packs are connected to the two-phase refrigeration cycle of the air conditioning system. Figure 17 shows a schematic diagram of such a system.

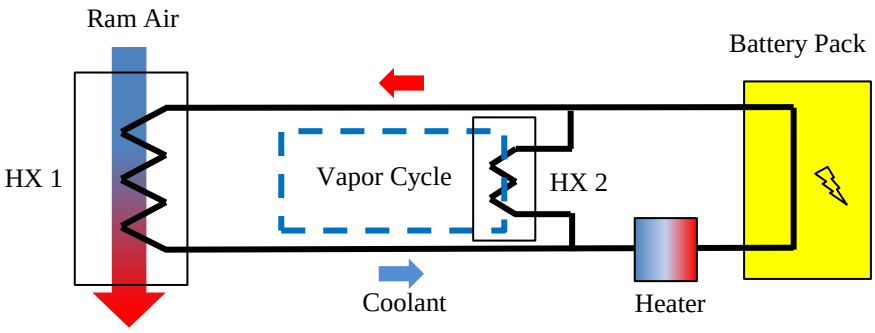

Figure 17: Simplified representation of the typical thermal management of a battery pack in a battery-electric car. At ambient temperatures below the battery operating temperature, the heat from the battery is dissipated via the first ram-air heat exchanger (HX 1). At ambient temperatures higher than the battery's operating temperature, the battery coolant temperature must be reduced via a second heat exchanger (HX 2), which is coupled to the air-conditioning systems vapor cycle.

The refrigeration cycle, which is on board of battery-electric cars, enables the battery to be cooled at ambient temperatures above the permissible battery temperature. Furthermore, the electric heater offers the possibility of regulating

DOI: 10.13009/EUCASS2023-463

the car battery at the ideal temperature level in cold ambient conditions. However, the refrigerant cycle of the car air conditioning system is not available onboard an aircraft. The aircraft environmental control system (ECS), which provides cooling at high ambient temperatures, typically is an air cycle machine instead of a two-phase vapor cycle as integrated in automobiles. The cooling circuit of the battery on the aircraft could be connected to the ECS at comparatively high cost. The battery and the ECS are safety relevant, therefore, combining functionalities would complicate the system design with respect to fault tolerance. The concept of a turbo-electric powertrain from a study by Perullo et al. for a regional jet envisages such an air-cooled battery in the lower fuselage deck [25]. The battery is tempered by the cold air from the ECS without the need to oversize the ECS. However, the ECS has to operate at full load during the entire mission to keep the battery below a selected maximum temperature of 45 °C. The latter leads to a block fuel increase of 1.4 %. In the study, the thermal capacity of batteries is relied upon to minimize the power consumption of the ECS at battery temperatures below 45 °C. The battery temperature remains above 40°C for most of the mission. However, the study does not address extreme load cases such as simultaneous air conditioning of the passenger cabin and fast charging of batteries on ground at hot day conditions.

If the thermal management system as proposed by Perullo et al. can meet all cooling and heating requirements and the battery pack weight does not exceed unreasonable values due to the disadvantages induced by air cooling, and if there are no other significant disadvantages with regard to aircraft integration i.e. a large increase in fuselage cross-section, this could be a synergetic solution. However, the integration of battery packs below the passenger cabin is questionable due to safety reasons (fire safety, crash safety) and might require costly provisions in terms of protection system mass. For the concept of this study, with battery packs distributed over the nacelles, the safety provisions might be relaxed due to the isolated integration under the wing. Nevertheless, for air-cooled battery packs, cold air from the ECS would have to be piped through the wings with the associated losses. Alternatively, liquid battery cooling could be enabled by a liquid-to-air heat exchanger that is closely integrated with the ECS. This booster function would be restricted to ground and low altitude flight load cases. In cruise flight, the ambient temperatures are low enough for air cooling via ram-air heat exchangers that are integrated closely to the battery packs in the nacelles. On the one hand, the power consumption of this heat transfer process is estimated to be high and might require an oversized ECS, on the other hand, the benefits of a liquid battery heat acquisition system might prevail. Replacing the air cycle of the ECS with a vapor cycle system (VCS) would require a special heat exchanger, as shown in Figure 17. Vapor cycle machines are more efficient than air cycle machines [26]. However, they are generally heavier and have not become widespread among airliners compared to the light and reliable air cycle systems [26,27]. A dedicated VCS for the battery is possible too. In a study conducted by Affonso et al. the aircraft maker Embraer selected a VCS in combination with a skin heat exchanger for any of the heat loads coming not only from the battery but also from electrical machines and power electronics [28]. The VCS is generally evaluated as mature and has been implemented in the aerospace industry [28].

Piezoelectric Heat Pump

A novel thermal management system for batteries is described in the study by Kellermann et al. [26]. There, the use of piezoelectric modules is proposed, which represent an electric heat pump without moving parts. A layout with heat pipes as heat acquisition system, and the integration of the piezoelectric modules into a plate heat exchanger, is able to operate without liquid coolants and other aggregates apart from a fan. The piezo modules are able to cool and also to heat and are easily controllable via the electrical power. The layout represents a highly integrated concept that has to be designed together with the battery housing and the arrangement of the cells. A quick estimate accounting for the estimated mass of the system using earlier derived penalty factors yields a block energy saving of 0.5 % at a mission distance of 400 nm. This assumes that half of the additional weight of the battery packs (interconnection of the individual cells, cooling ducts, coolant, housing, etc.) would be dropped and replaced by the piezoelectric system. Piezoelectric modules have not yet had any significance in aviation. Nevertheless, this approach offers an alternative that could be investigated in more detail.

Mobile Ground Unit

The options described above show possibilities to design a cooling system that can deal with all environmental conditions by itself. However, the question arises whether this flexibility is necessary. The fast charging infrastructure, including intermediate storage, for an aircraft with MWh-sized batteries is already a challenge itself and will be an expensive investment for airports planning to handle a hybrid-electric regional aircraft. Given the unfavorable boundary conditions for battery cooling, which are primarily encountered on the ground, there would be an opportunity to provide the required cooling power through ground infrastructure. As of today, conditioned air is provided to large commercial aircraft at the gate so that less fuel is burned in the inefficient APU to provide the power for air conditioning and to improve local air quality. A mobile charging station with an integrated vapor cycle to support battery cooling would greatly simplify systems on the aircraft and reduce costs. Installing a heat pump on a truck is much less expensive than on an aircraft. This external cooling unit would pre-cool the batteries via a central system so that the thermal capacity of the batteries would be sufficient to bear the waste heat of the short taxi and take-off phase. The discussed options for battery thermal management are summarized in Table 5.

DOI: 10.13009/EUCASS2023-463

Table 5: Options for battery thermal management system with qualitative remarks

Battery Cooling	Heat Pump	Comment
Liquid	Air Cycle ECS	• Possibly oversizing of the ECS for additional load cases • Inefficient heat transfer between air cycle machine and liquid battery coolant
Air	Air Cycle ECS	• Possibly oversizing of the ECS for additional load cases • Higher battery pack weight and larger volume due to air-based heat acquisition system
Liquid	Vapor Cycle ECS	• Possibly oversizing of the ECS for additional load cases • Improved heat transfer between vapor cycle refrigerant and liquid battery coolant • Vapor cycle is more efficient but the system is heavier and unusual for the ECS application
Liquid	Vapor Cycle	• Mature technology
Heat Pipes	Piezoelectric Modules	• Decentralized, lightweight and easily controllable system • Highly integrated, specialized concept • Unconventional, no experience with piezoelectric modules in aviation
Liquid	Ground Based Unit	• Simplest and cheapest system on aircraft level • No autonomy in case of missing airport infrastructure

The project consortium opted for a liquid-cooled battery with a mobile, ground-based heat pump. This option reduces the complexity of the overall system, still offers flexibility in the design of the heat exchangers and promises good overall efficiency at airplane level. In the current model, the heat exchangers are not specifically designed for their respective applications. Instead, the rejected heat is divided by a factor given in Table 6 to obtain the total cooling system mass and thus to account for the general mass impact of the cooling system. The battery cooling air drag is neglected as well.

4.9 Comparison with the Baseline Aircraft

The previous chapters described individual aspects of the aircraft and the propulsion architecture. The final, energetic comparison between the HEP architecture and conventional baseline distances is shown along with relative fleet frequency over various mission distances in Figure 18. The diagram shows the optimum hybridization level identified from Figure 14 with a battery pack that allows for 213 nm all-electric range (i.e. 8000 kg battery pack).

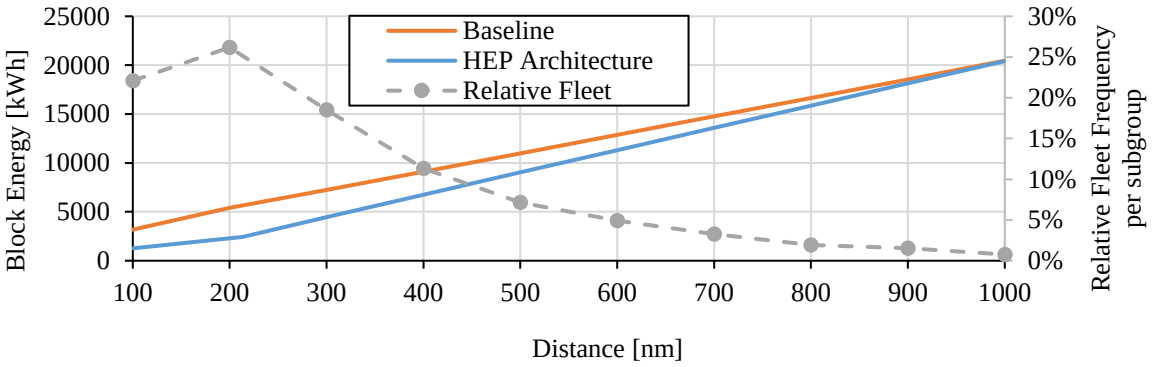

Figure 18: Block energy consumption of the hybrid-electric design with 46 % hybridization compared to the conventional baseline. Furthermore, the relative fleet frequency distributed over the distances is plotted. The dots represent the relative amount of flights per subgroup, e.g., “from 0 to 100 nm” or from “100 to 200 nm” distance etc.

The maximum take-off mass increases by 43.9 % versus the baseline. The relative fleet frequencies shown in Figure 18 indicate the dominance of the very short ranges i.e. the peak group at ranges from 100 to 200 nm. The group around 0nm (aerodrome circuits etc.) is not shown as it drops to only 2.4 % of the mission mix. At 200 nm distance, the HEP architecture achieves a block energy reduction of 57.4 % versus the baseline. Above the battery-electric range of 213 nm, the advantage of the HEP architecture decreases as the fuel burning range extender has to be turned on. Therefore, the gradient of the energy consumption is higher past the battery-electric range. At 400 nm, there are still 25.9 % energy savings, and at the design range of 1000 nm, the difference becomes negligible. Considering the fleet, the

DOI: 10.13009/EUCASS2023-463

hybrid-electric design can achieve energy savings of about 34.6 % and fuel savings of 64.4 %. The reasons for this performance are due to the following key aspects in the given order:

- Fully battery-electric concept, implying high efficiency of battery, electrical machines and power electronics
- Utilization of the battery energy only for the main mission, not for the reserves
- Serial hybrid-electric architecture
    - Higher efficiency and lower weight of a single gas turbine as range extender
    - Distributed propulsion
        - Lower installed power-to-mass ratio due to increased redundancy compared to twin-engine
        - Improved propeller efficiency (10 versus 2 propellers)
        - Higher wing-loading in cruise due to smaller wing (improved low-speed performance)
        - Synergistic integration of the battery packs in engine nacelles with little increase in wetted area and additional wing bending relief
        - Low-wing configuration for minimized drag and relief of the fuselage structure

5. Conclusions and Outlook

In the present paper, a number of architecture trade-offs have been performed on aircraft level. The initial selection of the plug-in concept with a range extender makes up the dominant benefit. The subsequent trade-offs further enhance the overall potential of this concept. The low-wing configuration was found to be the best wing integration option as the distributed electric propulsion opens new possibilities with smaller propellers. The number of propellers was optimized to ten same sized propellers. However, the pool of methods for this comparison lack in the level of detail in order to make an informed decision on this specific aspect. Furthermore, as the results showed, the number of propellers may not be the decisive factor in the overall performance. The optimal number of range extenders was clearly identified to be a singular one, that is integrated in one of the inner nacelles. The higher efficiency, lower weight and less cost of one large gas turbine versus two smaller ones of the same total power are enabled by the choice of a serial-hybrid electric architecture.

The factors that influence the optimal pack size are the fleet mission mix and the energy costs. At low fuel costs the smaller packs are obviously preferred. Considering a future scenario when electricity from renewable energy will always be cheaper than synthetic air fuels (SAF) produced from that same energy, it is clear that a larger battery pack will save costs up to the point when it impairs the overall aircraft performance. Operational factors such as constraints on the turnaround-time at the airport and limitations to charging power may also influence the decision on battery pack size. The thermal management was found to be manageable with conventional liquid cooling for most of the electric components such as the generator, e-motors and power electronics. The battery packs though require special cooling equipment due to their narrow allowable temperature spectrum. The fast charging on ground on a hot day was identified to be the sizing condition for the system. Several options for a heat pump were discussed and eventually a ground-based, external solution selected. The disadvantage in operative autonomy was accepted as the aircraft performance is expected to be the best achievable one. The final comparison between the optimized hybrid-electric architecture showed a fleet-level energy reduction of 34.6 % and a fuel reduction of 64.4 %.

The trade-offs performed in this study were based on classic handbook methods for conceptual aircraft design, fixed inputs for hybrid-electric components and many other simplifications. The volumes of battery packs, heat exchangers and other electrical components in the nacelles were roughly estimated without a detailed check on the installation space. These simplifications were made to identify the overall optimal configuration for the hybrid-electric architecture. The results present an intermediate status of the project and will be updated by ongoing investigations on specific nacelle geometries and electrical components. Furthermore, a study on the direct operating costs including the electric components will provide another criterion that will aide in the task to identify the optimal architecture.

6. Annex

The year 2035 was set in the project TELEM as year of entry-into-service and with it the expected component technology level of that year. The generator design for the range extender was investigated by the project partner Rolls Royce Electrical [29]. The resulting power specific mass and the efficiency were used as a fixed input for the aircraft level studies. The assumptions on the geared electrical motor, power electronics and power cables are initial values retrieved from internal data and will be updated in the next project phase. The numbers are given in Table 6. The battery assumptions were derived from the roadmap published by the Strategic Research Agenda [30] for high-energy aircraft batteries available in the year 2030 with a performance penalty due to conservatism. The usable state-of-charge is set between 90 % and 0 % after taxi-in. The 90 % account for battery ageing. The 0 % represents an optimistic assumption. If additional reserves are considered, the battery-electric range is reduced nearly linearly and the energy benefit against the conventional baseline will decrease accordingly. The cables have a specific power of 700 kWm/kg with an efficiency reduction of 0.02 % per meter. An installation factor of 2 is applied for the mass and efficiency of the power transmission after calculating the cable length (to account for more complex routing).

DOI: 10.13009/EUCASS2023-463

Table 6: Assumptions for power densities of electrical machines and the heat per kg rejected by a liquid cooling system

Component	Power/Heat [kW/kg]	Efficiency [%]
Geared E-Motor	10	98
Inverter	60	98.5
Rectifier	60	98.4
Generator	16	98.5
Liquid Cooling System (incl. heat exchanger, fluids, pumps, pipes)	1.6	-

Table 7: Assumptions for battery utilization and specific energy density

Sp. Energy (Cell Level)	Wh/kg	400
Sp. Energy (Cell Level)	Wh/l	850
Starting State of Charge (before mission)	%	90
End SoC (after mission)	%	0
Cell-to-Pack Gravimetric Ratio	-	0.8
Cell-to-Pack Volumetric Ratio	-	0.75
Pack-level grav. energy density	Wh/kg	320
Pack-level vol. energy density	Wh/l	637.5
Pack-level density	kg/l	1.99

7. Acknowledgements

The input from Wolfgang Grimme (DLR Institute for Air Transport and Airport Research) on the turn-around times of regional aircraft is appreciated.

The work was supported by the Federal Ministry for Economic Affairs and Climate Action as per resolution of the German Bundestag under grant number 20M1916F.

Supported by:

Federal Ministry
for Economic Affairs
and Climate Action

on the basis of a decision
by the German Bundestag

8. References

[1] Strack, M., Pinho Chiozzotto, G., Iwanizki, M., Plohr, M., and Kuhn, M., "Conceptual Design Assessment of Advanced Hybrid Electric Turboprop Aircraft Configurations," *17th AIAA Aviation Technology, Integration, and Operations Conference*, 17th AIAA Aviation Technology, Integration, and Operations Conference, Denver, Colorado, American Institute of Aeronautics and Astronautics, Reston, Virginia, 2017. doi: 10.2514/6.2017-3068

[2] Voskuijl, M., van Bogaert, J., and Rao, A. G., "Analysis and design of hybrid electric regional turboprop aircraft," *CEAS Aeronautical Journal*, Vol. 9, No. 1, 2018, pp. 15–25. doi: 10.1007/s13272-017-0272-1

[3] Spierling, T. and Lents, C. E., "Parallel Hybrid Propulsion System for a Regional Turboprop: Conceptual Design and Benefits Analysis," *AIAA Propulsion and Energy 2019 Forum,* AIAA Propulsion and Energy 2019 Forum, Indianapolis, IN, American Institute of Aeronautics and Astronautics, Reston, Virginia, 2019. doi: 10.2514/6.2019-4466

[4] Finger, D. F., Vries, R. de, Vos, R., Braun, C., and Bil, C., "A Comparison of Hybrid-Electric Aircraft Sizing Methods," *AIAA Scitech 2020 Forum,* AIAA Scitech 2020 Forum, Orlando, FL, American Institute of Aeronautics and Astronautics, Reston, Virginia, 2020. doi: 10.2514/6.2020-1006

DOI: 10.13009/EUCASS2023-463

[5] Antcliff, K. R., Guynn, M. D., Marien, T., Wells, D. P., Schneider, S. J., et al., "Mission Analysis and Aircraft Sizing of a Hybrid-Electric Regional Aircraft," *54th AIAA Aerospace Sciences Meeting,* 54th AIAA Aerospace Sciences Meeting, San Diego, California, USA, American Institute of Aeronautics and Astronautics, Reston, Virginia, 2016. doi: 10.2514/6.2016-1028

[6] Atanasov, G., van Wensveen, J., Peter, F., and Zill, T., "Electric Commuter Transport Concept Enabled by Combustion Engine Range Extender," *Deutscher Luft- und Raumfahrtkongress 2019,* Deutsche Gesellschaft für Luft- und Raumfahrt - Lilienthal-Oberth e.V., 2019. doi: 10.25967/490245

[7] Atanasov, G., "Potential Propulsion Architecture for a Reduced Climate Impact of Civil Aviation," *E2Flight 2020,* Stuttgart, 20.-21.02.2020, 2020.

[8] Atanasov, G., "Comparison of Sustainable Regional Aircraft Concepts," *Deutscher Luft- und Raumfahrtkongress 2022,* Deutsche Gesellschaft für Luft- und Raumfahrt - Lilienthal-Oberth e.V., 2022.

[9] Wassink, P., Atanasov, G., Hesse, C., and Fröhler, B., "Conceptual Design of Silent Electric Commuter Aircraft," *ICAS 2021 - 32nd Congress of the International Council of the Aeronautical Sciences. September 6-10, 2021, Pudong Shangri-La, Shanghai, China,* The International Council of the Aeronautical Sciences, 2021.

[10] Woehler, S., Atanasov, G., Silberhorn, D., Froehler, B., and Zill, T., "Preliminary Aircraft Design within a Multidisciplinary and Multifidelity Design Environment," *Aerospace Europe Conference 2020,* 2020.

[11] Boden, B., Flink, J., Först, N., Mischke, R., Schaffert, K., et al., "RCE: An Integration Environment for Engineering and Science," *SoftwareX,* Vol. 15, 2021, p. 100759. doi: 10.1016/j.softx.2021.100759

[12] Alder, M., Moerland, E., Jepsen, J., and Nagel, B., "Recent advances in establishing a common language for aircraft design with CPACS," *Aerospace Europe Conference 2020,* 2020.

[13] Schroeter, J., "TELEM Co-Memo Nr. 2 [Internal Document]," 2021.

[14] Schroeter, J., "TELEM Co-Memo Nr. 5 [Internal Document]," 2022.

[15] Biser, S., Atanasov, G., Hepperle, M., Filipenko, M., Keller, D., et al., "Design Space Exploration Study and Optimization of a Distributed Turbo-Electric Propulsion System for a Regional Passenger Aircraft," *AIAA Propulsion and Energy 2020 Forum,* VIRTUAL EVENT, American Institute of Aeronautics and Astronautics, Reston, Virginia, 2020. doi: 10.2514/6.2020-3592

[16] Fröhler, B., Hesse, C., Atanasov, G., and Wassink, P., "Disciplinary Sub-Processes to Assess Low-Speed Performance and Noise Characteristics within an Aircraft Design Environment," *Deutscher Luft- und Raumfahrtkongress 2020,* Deutsche Gesellschaft für Luft- und Raumfahrt - Lilienthal-Oberth e.V., 2020.

[17] Keller, D., "Towards higher aerodynamic efficiency of propeller-driven aircraft with distributed propulsion," *CEAS Aeronautical Journal,* Vol. 12, No. 4, 2021, pp. 777–791. doi: 10.1007/s13272-021-00535-5

[18] Roskam, J., *Airplane design. Part V: Component Weight Estimation,* 3rd ed., DARcorporation, Lawrence, Kansas, 2003.

[19] Geiß, I. and Strohmayer, A., "Operational Energy and Power Reserves for Hybrid-Electric and Electric Aircraft," *Deutscher Luft- und Raumfahrtkongress 2020,* Deutsche Gesellschaft für Luft- und Raumfahrt - Lilienthal-Oberth e.V., 2020. doi: 10.25967/530149

[20] Starke, M., Moorthy, R. S. K., Adib, A., Dean, B., Chinthavali, M., et al., "A MW scale charging architecture for supporting extreme fast charging of heavy-duty electric vehicles," *2022 IEEE Transportation Electrification Conference & Expo (ITEC),* 2022 IEEE/AIAA Transportation Electrification Conference and Electric Aircraft Technologies Symposium (ITEC+EATS), Anaheim, CA, USA, 15.06.2022 - 17.06.2022, IEEE, 2022, pp. 485–490. doi: 10.1109/ITEC53557.2022.9813825

[21] "Pipistrel Alpha Electro," URL: https://www.emobility-engineering.com/pipistrel-alpha-electro/ [retrieved 16 May 2023].

[22] Pipistrel d.o.o, "Pipistrel Velis Electro," URL: https://www.pipistrel-aircraft.com/products/general-aviation/velis-electro/ [retrieved 16 May 2023].

[23] An, Z., Jia, L., Ding, Y., Dang, C., and Li, X., "A review on lithium-ion power battery thermal management technologies and thermal safety," *Journal of Thermal Science,* Vol. 26, No. 5, 2017, pp. 391–412. doi: 10.1007/s11630-017-0955-2

[24] Annapragada, R., Sur, A., Mahmoudi, R., Macdonald, M., and Lents, C. E., "Hybrid Electric Aircraft Battery Heat Acquisition System," *2018 AIAA/IEEE Electric Aircraft Technologies Symposium,* 2018 AIAA/IEEE Electric Aircraft Technologies Symposium, Cincinnati, Ohio, American Institute of Aeronautics and Astronautics, Reston, Virginia, 2018. doi: 10.2514/6.2018-4992

[25] Perullo, C., Alahmad, A., Wen, J., D'Arpino, M., Canova, M., et al., "Sizing and Performance Analysis of a Turbo-Hybrid-Electric Regional Jet for the NASA ULI Program," *AIAA Propulsion and Energy 2019 Forum,* AIAA Propulsion and Energy 2019 Forum, Indianapolis, IN, American Institute of Aeronautics and Astronautics, Reston, Virginia, 2019. doi: 10.2514/6.2019-4490

[26] Kellermann, H., Fuhrmann, S., Shamiyeh, M., and Hornung, M., "Design of a Battery Cooling System for Hybrid Electric Aircraft," *Journal of Propulsion and Power,* Vol. 38, No. 5, 2022, pp. 736–751. doi: 10.2514/1.B38695

DOI: 10.13009/EUCASS2023-463

[27] Pérez-Grande, I. and Leo, T. J., “Optimization of a commercial aircraft environmental control system,” *Applied Thermal Engineering*, Vol. 22, No. 17, 2002, pp. 1885–1904. doi: 10.1016/S1359-4311(02)00130-8
[28] Affonso, W., Tavares, R., Barbosa, F. R., Gandolfi, R., dos Reis, R. J. N., et al., “System architectures for thermal management of hybrid-electric aircraft - FutPrInt50,” *IOP Conference Series: Materials Science and Engineering*, Vol. 1226, No. 1, 2022, p. 12062. doi: 10.1088/1757-899X/1226/1/012062
[29] Biser, S., “Generator Design: TELEM 70 PAX Aircraft [Internal Document],” 2022.
[30] European Technology and Innovation Platform on Batteries - Batteries Europe, “Strategic Research Agenda,” 2020.